Design, Synthesis, and Biological Evaluation of Metal-Based Schiff Base Complexes of Cephalosporins and Aldehydes for Enhanced Bioavailability and Resistance Modulation

Naeem Razaq[1], Amina Asghar[2]*, Amina Mumtaz[3], Mehr un Nisa[4], Bilal Shahid[5], Muhammad Zahid Qureshi[6]*

[1]Department of Chemistry, Division of Science and Technology, University of Education, Township, Lahore, 54770, Pakistan. Email: naeemchem90@gmail.com
[2]Department of Chemistry, Division of Science and Technology, University of Education, Township, Lahore, 54770, Pakistan. Email: amina.asghar@ue.edu.pk
[3]Applied Chemistry Research Center, PCSIR Laboratories Lahore, Lahore, Pakistan. Email: amina.mumtaz@hotmail.com
[4]Department of Chemistry, University of Lahore, Lahore, Pakistan. Email: mehr.nisa@chem.uol.edu.pk
[5]Department of Chemistry, Division of Science and Technology, University of Education, Township, Lahore, 54770, Pakistan. Email: bilalshahid_1@hotmail.com
[6]College of Agriculture and Food, Department of Environment and Natural Resources, Qassim University, Buraidah 52454, Saudi Arabia. Email: m.qureshi@qu.edu.sa

Abstract

Background: To boost therapeutic efficiency against bacterial species that repeatedly resist the medical treatment, Schiff basis are the key area of focus for currently available antimicrobial medications that has to be carefully researched. In this study, we have concentrated on a unique and ecologically benign condensation reaction approach that offers both higher biological efficacy and "green synthesis as well". **Methods:** Hence, in this study, transition metal (opper (II), manganese (II), iron (II), nickel (II), and zinc (II) complexes of cefixime with well-improved biological activities were synthesized. The products were characterized by employing UV-Visible spectroscopy, elemental analysis, Fourier-transform infrared spectroscopy (FT-IR), proton nuclear magnetic resonance spectroscopy (^{1}H-NMR), inductively coupled plasma optical emission spectroscopy (ICP-OES), and powder X-ray diffraction (XRD. The products were assessed for their in-vitro anti-inflammatory activities utilizing protein denaturation as well as proteinase inhibiting assays. The *in-vitro* antioxidant activity of the products was determined by utilizing the 2,2-diphenyl-1-picrylhydrazyl (DPPH) *in-vitro* method. The biological studies were carried out by utilizing in-vitro anti-bacterial investigation with the disc diffusion method. **Results:** The results attributed the metal complexes to be more efficient against bacterial germs as compared to respective parent medicines and their free ligands as well. In *silico* studies were also carried out on the basis of hydrogen bond interactions, complex A5, with a binding energy of -8.9 kcal/mol, was found to have the strongest antibacterial activity among complexes A1, A2, A3, A4, A5, and ligand AL. **Conclusion:** These findings are very encouraging and well positioned to open the horizons for further research in this diverse field.

Keywords: Synthesis, Biological Activity, Microorganisms, Antioxidant, Metal Complexes, Nutrition Plates.

Introduction

In current times, it has become inevitable to study and establish a new generation of antimicrobial medications that can effectively treat microbial infections which are resistant to many medications. There have been various methodologies employed to enhance the bactericidal efficacy of antibiotics. One of such strategies is based on coordinating metal ions with ligands containing antibiotics that show significant potential in combating various bacterial strains. Moreover, transition metal complexes generally display a diverse range of coordination characteristics and bioactivities, along with the capacity to establish distinctive reaction to various biomolecules. The term "β-lactam antibiotics" refers to the basic chemical

Access This Article Online

Quick Response Code:

Website: www.jnsbm.org

DOI: https://doi.org/10.5281/zenodo.19550924

Address for Correspondence: Department of Chemistry, Division of Science and Technology, University of Education, Township, Lahore, 54770, Pakistan
Email: amina.asghar@ue.edu.pk
College of Agriculture and Food, Department of Environment and Natural Resources, Qassim University, Buraidah 52454, Saudi Arabia
Email: m.qureshi@qu.edu.sa

Submitted: 05th January, 2026 **Received:** 13th January, 2026
Accepted: 01st March, 2026 **Published:** 09th March, 2026

How to Cite This Article: Razaq N, Asghar A, Mumtaz A, Nisa M U, Shahid B, Qureshi M Z. Design, Synthesis, and Biological Evaluation of Metal-Based Schiff Base Complexes of Cephalosporins and Aldehydes for Enhanced Bioavailability and Resistance Modulation. J Nat Sc Biol Med 2026;17(1):37-55

structure of the resulting drugs with β-lactam ring being the main part of them. This ring plays an important part for the antibacterial activity of the β-lactam antibiotics, when it is disrupted, the β-lactams lose their efficacy.

β-lactamase enzyme activity is another widely described process of the resistance. The fundamental issue in antibiotic treatment resides in the vulnerability to the activities of β-lactamases. The bacterial enzymes possess the β-lactam ring, which leads to the irreversible deactivation of the antibiotic and the consequent loss of its potency.[1]

Antibiotic resistance mechanisms in bacteria are as follows: (i) structures alterations on the antibiotic focused site; (ii) substitution of the original target region with new molecules that do not bind to the antibiotics; (iii) decreased antibiotic permeation of the cell membrane; and (iv) active discharge of the antibiotics from the cells themselves. The application of the biological and diagnostic properties of metal ions is one of the methods for altering the antibiotics. These ions can form complex molecules by interacting with penicillin derivatives, which act as a barrier to prevent the β-lactam ring from opening.[2]

According to the original description by Hugo Schiff about 160 years ago, Schiff base has been referred to as "Schiff" ever since. Schiff bases play an important functional part as ligands, which are among the most often used organic compounds, even though if these were found in coordination chemistry about a century ago.[3] Recently, due to significant applications in analytical chemistry, the organic synthesis and refinement of metals, the electroplating process, metalworking, and in photography, Schiff-based chemistry for coordination has gained a great interest. Schiff bases serve key roles in current chemistry of coordination as well as in the advancement of bioinorganic chemistry.[4]

These substances are useful in treating a variety of diseases other than microbial infections due to their anti-microbial action. Metal carrier medications are believed to be simple carriers that can achieve quick fluids and lipids dissolvability, penetration, bioavailability, and controlled drug administration. These may additionally initiate pharmacokinetic changes. Schiff bases with donor groups play a significant role in bioinorganic chemistry, producing stabilized metal complexes with a range of metal ions.[5]

There have been various names for Schiff bases like imine, anil, or azomethine, but the azomethine group (R1R2C=NR3) represents the most prevalent structural characteristic of Schiff bases, whereas substitutions might be heterocyclic, aryl, cycloalkyl, or an alkyl group. Heteroatoms such as oxygen, sulphur, and nitrogen are often utilized in metal-binding reactions with ligands. A coordination complex is generated when a coordination bond is established between the metal and the ligand. Throughout human history, metals and their derivatives have been utilized extensively in medicine.[6] Schiff bases metal complexes possess a broad range of biological activities as analgesics, anti-inflammatory, anticancer, antibacterial, antifungal drugs, etc. However, there are certain drugs that have demonstrated to operate better when supplied as metal complexes than free chemical components. Due to the lone pair electrons assistance to bind proteins in live organisms, the existence of these electrons is connected to the potential biological activities of Schiff base metal complexes. Due to the generation of β-lactamases enzymes, the majority of penicillin treatments have been demonstrated to be resistant to some hazardous bacterial strains. However, when these antibiotics are coupled with metal complexes, their antibacterial activities are boosted. Schiff base ligands based on penicillin are versatile pharmacophores that give a simple template for binding a range of metal ions.[7]

Although, there are certain forms of cephalosporins that have been proven effective towards Gram-negative bacteria, but most of the original cephalosporins are effective against Gram-positive bacteria. Despite an increase in the usage of broad-spectrum cephalosporins, resistance of cephalosporins remains. The mold Cephalosporin acremonium produces natural antibiotic cephalosporin, which is the source of the semisynthetic cephalosporin antibiotics. The antibiotics and penicillin are related to one another. Its resistance mechanisms, way of action, and a few other features are completely same. The β-lactam antibiotic class comprises both cephalosporins and penicillin. Based on their range of actions, cephalosporins are categorized into four generations. When it comes to Gram-positive *cocci*, the first generation cephalosporins are highly effective. Their potency against Gram-negative bacteria is constrained.[8]

The third-generation cefixime is a semisynthetic cephalosporin antibiotic that is 7-2(2-(amino-4-thiazolyl)-2(carboxymethoxyimino) acetamido) -3-vinyl-cephem4-carboxylic acid. It functions stronger against bacteria that are gram negative and less effectively against the gram-positive. But the continued consumption of these wide range spectrum antibiotics raises concerns since it encourages the spread of illnesses that are difficult to cure and resistant to many drugs.[9]

Cefixime, since it combines both structural and biological changes brought about by Schiff base formation and metal complexation with the pharmacological potential of cefixime, a third-generation cephalosporin antibiotic. Cefixime Schiff base metal complexes are an intriguing area of study. Against both Gram-positive and Gram-negative bacteria, cefixime exhibits strong action. Improved action against both common and resistant bacteria is demonstrated by cefixime metal complexes.[10]

Cefixime's cytotoxic or antimicrobial effects of many β-lactam-derived complexes can be explained by the way that metal coordination alter binding to bacterial enzymes (like penicillin-binding proteins or other metalloenzymes) and facilitate or enhance interactions with nucleic acids (intercalation or groove binding). Several experimental articles include enzymatic inhibition experiments and spectroscopic DNA-binding studies.[11]

Vanillin itself shows mild antibacterial and antifungal

properties (phenolic OH and aldehyde group disrupt microbial cell walls/proteins). Schiff base formation (usually with amines) and coordination with metals (Cu(II), Zn(II), Co(II), Ni(II), Fe(III), etc.) greatly enhances antimicrobial efficacy. Metal complexes are more lipophilic → easier penetration into bacterial membranes. Some also generate reactive oxygen species (ROS) that damage microbes.[12]

Materials and Methods

The analytical grade solvents and reagents were purchased from Merck and VWR. Pure raw cephalosporin drugs are bought from Star Laboratories, Lahore, Pakistan. Prior to usage, the solvents were redistilled by using standard techniques.

Characterization

The Stuart SMP11 Analogue Melting Point equipment was used to determine the decomposition and melting points of the ligand and metal complexes as well with an accuracy of 0.01°C. The diffracted intensities of the complexes were obtained by the utilization of an Ultima IV X-ray diffractometer (Rigaku model, CuKa 14 = 0.1540562 nm). The Perkin Elmer Spectrum 3 FTIR imaging Spectrometer featuring ATR assembly was utilized to obtain the FTIR spectra. The UV-visible spectra of all the products were acquired at room temperature by employing the Shimadzu 2600i spectrophotometer. The (C, N, and H %) of newly synthesized complexes were ascertained by using a 2500 series elemental analyzer (Perkin Elmer, USA). The metal contents of the complexes were determined by using the ICP-OES7000 Series (Agilent Technologies, USA).

Ligand Synthesis (FL)

Both vanillin and cefixime (10mM) solutions were made by using molar ratio of 1:1. Later, it was poured in a 250mL round bottomed flask and mixed to make a homogenous solution. The Vanillin ethanolic solution was made in 50 mL of ethanol by dissolving 0.071g vanillin and methanolic solution of drug was prepared by dissolving 0.453 grams of cefixime in 50 mL of methanol. Sodium Hydroxide (NaOH) (1M) solution was used to regulate the pH around 7-8 to the mixture solution. The solution was refluxed at 60–70 °C for three to five hours with constant magnetic stirring. The final synthesized product was a clear solution with a brownish color, and the Schiff base ligand crystals were produced after evaporation. The freshly prepared and dried crystalline product was stored in a vacuum-sealed desiccator. The purity of the ligand was determined by using Thin-Layer Chromatography (TLC).

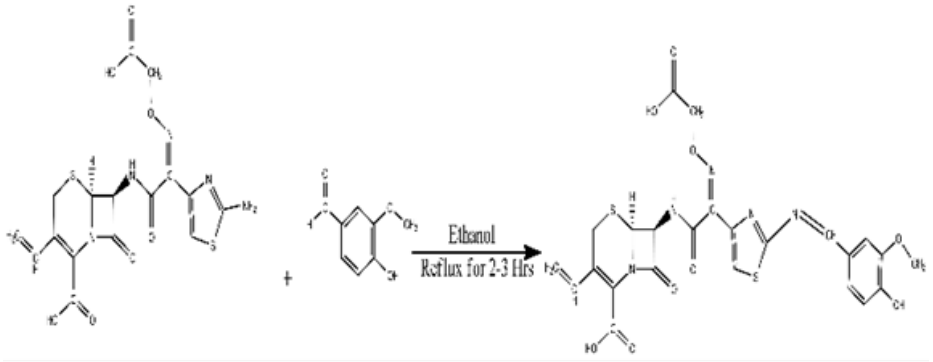

Cefixime Vanillin Proposed Structure ofVanillidenecefixime

(6S,7S)-7-((Z)-2-((carboxymethoxy)imino)-2-(2-((E)-(4-hydroxy-3-methoxybenzylidene) amino)thiazol-4-yl) acetamido)-8-oxo-3-vinyl-5-thia-1-azabicyclo[4.2.0]oct-2-ene-2 carboxylic acids

[$C_{24}H_{27}N_5O_{12}S_2$] Yield: 79%; M.P.: 200 C; Color: Brown; UV-Vis (DMSO): 337-372 (π →π*, n→π*) (-C=N azomethine); FTIR (KBr, cm^{-1}): 1630 ν(-C=N) (azomethine), 3375 ν(–OH), 1770 ν(-C=0)β- lactam, 1257 ν(C-O), 1455 ν(COO) (symt); ^{1}H-NMR (500 MHz, DMSO-d6): 3.60–3.79 (3H, d, –OCH3), 9.71 (1H, s, OH), 6.76-6.84 (1H, d, β-lactam), 8.35 (1H, s, CH=N), 2.45–2.48 (3H, d, –CH3): LCMS: $[M]^+$, $[C_{24}H_{27}N_5O_{12}S_2]^+$, 641 m/z (calculated. 641.76 m/z); Elemental analysis, found (calc.): C 44.76% (44.88%), H 4.18% (4.20%), N 10.90% (11.02%).

Schiff Base Metal (II) Complexes Synthesis

Cefixime and vanillin's condensation reaction product was subsequently mixed with appropriate metal salts of Cu (II), Ni (II), Mn (II), Zn (II) and Fe (II) by using the molarity ratio of 1:2 (metal: ligand) for the formation of Schiff base metal complexes. For 3-4 hours, the aqueous metal solution of metals (20 mmol) was reacted with newly prepared Schiff base ligand. After refluxing and magnetically stirring the reaction solution at 56–66 °C, it resulted in formation of Schiff base metal complexes with a variety of colors. The evaporation method was used to precipitate out the Schiff base complexes. The newly formed crystallized products were air-dried and stored at room temperature in a vacuum-sealed desiccator. Each products were tested for purity using TLC.

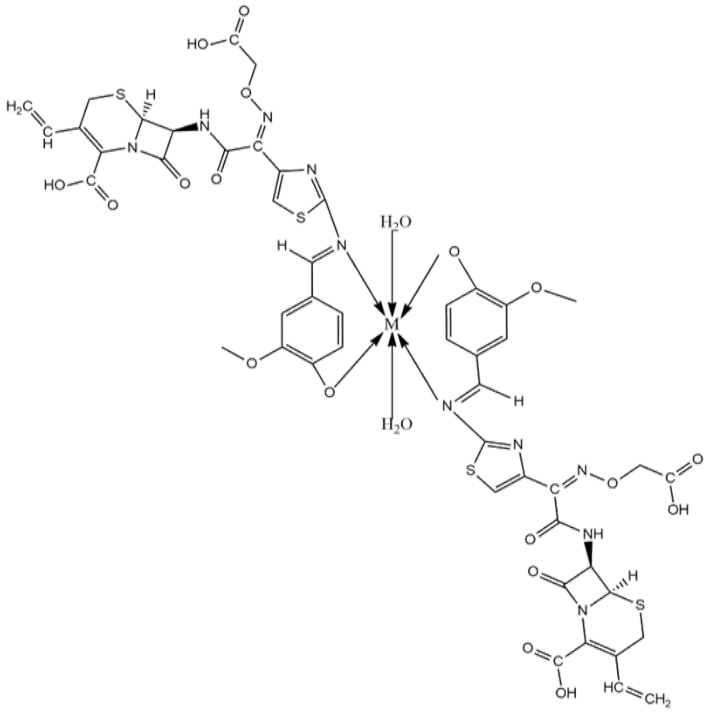

Proposed structure of metal complexes
Where M is Fe, Cu, Ni. Mn, Zn:

$[Fe(L\text{-}H)_2(H_2O)_2]$

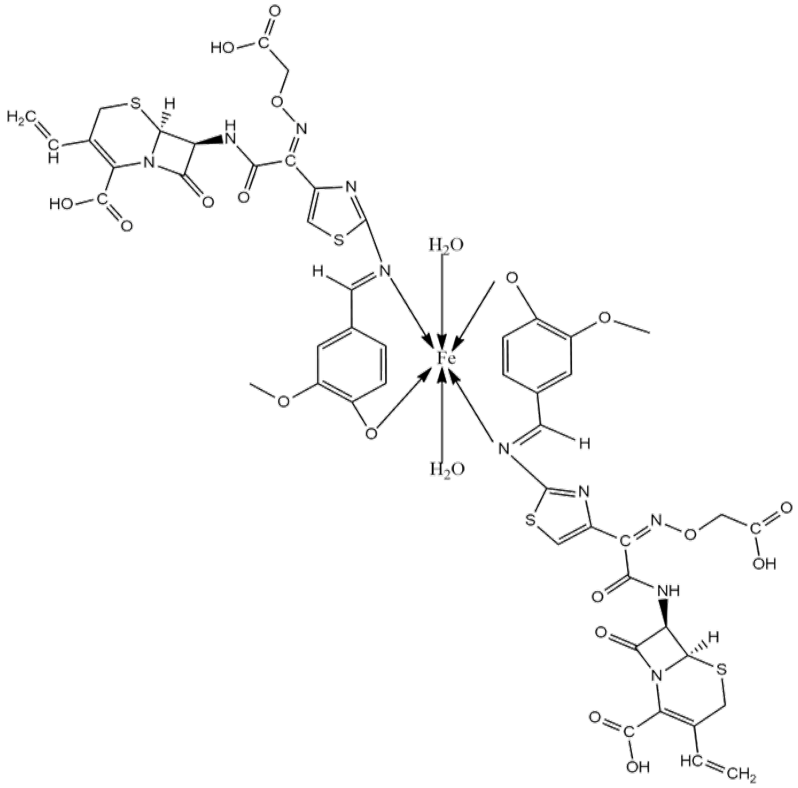

Red solid of $C_{48}H_{58}N_{10}0_{26}S_4Fe$; Yield (71%); M.W (1375.14); UV-Vis (DMSO): 415-460 L-M-OH ($\pi \rightarrow \pi^*$, d→d); FTIR (KBr, cm^{-1}): 436 (M-O), 1657 (-HC=N), 555 (M-N), 3214 (-OH), 1738 (-C=O β-lactam), 1583 (-COO); OCP-OES and Elemental analysis, found (calc.): C 41.97% (41.88%), H 41.88% (4.21%), N 10.22% (10.18%), Fe 4.11% (4.06%)

$[Cu(L\text{-}H)_2(H_2O)_2]$

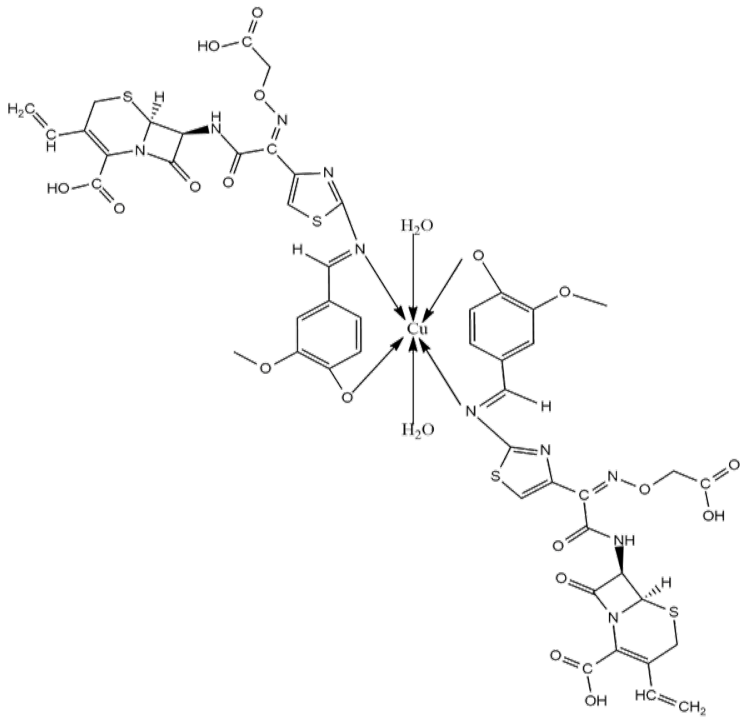

Brown solid of $C_{48}H_{58}N_{10}0_{26}S_4Cu$; Yield (73%); M.W (1382.83); UV-Vis (DMSO): 421-457 L-M-OH ($\pi \rightarrow \pi^*$, d→d); FTIR (KBr, cm^{-1}): 1664 (-HC=N), 432 (M-O), 561 (M-N), 3185 (-OH), 1744 (-C=O β-lactam), 1590 (-COO); OCP-OES and Elemental analysis, found (calc.): C 41.37% (41.60%), H 4.23% (4.19%), N 10.19% (10.13%), Cu 4.71% (4.59%)

$[Ni(L\text{-}H)_2(H_2O)_2]$

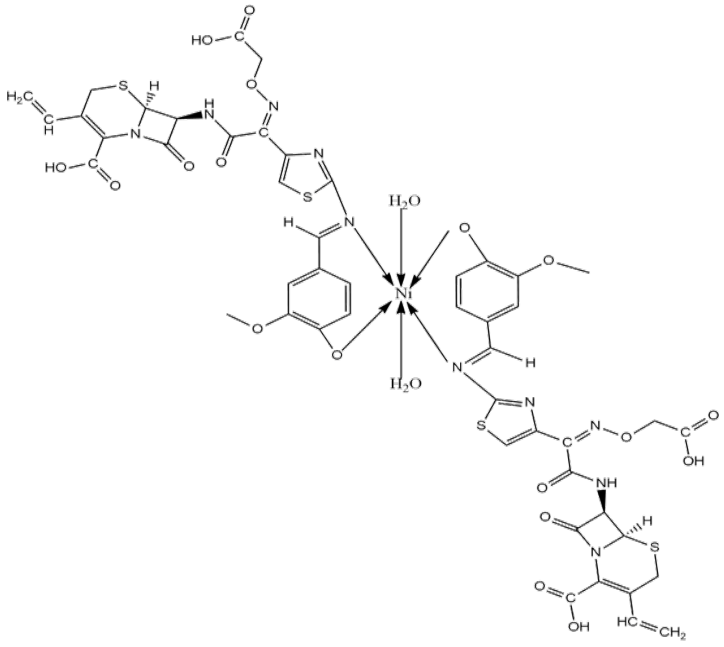

Brown solid of $C_{48}H_{58}N_{10}0_{26}S_4Ni$; Yield (77%); M.W (1377.99); UV-Vis (DMSO): 407-453 L-M-OH ($\pi \rightarrow \pi^*$, d→d); FTIR (KBr, cm^{-1}): 1659 (-HC=N), 438 (M-O), 557 (M-N), 3188 (-OH), 1738 (-C=O β-lactam), 1581 (-COO); OCP-OES and Elemental analysis, found (calc.): C 41.92% (41.83%), H 4.28% (4.21%), N 10.23% (10.16%), Ni 4.34% (4.26%)

$[Mn(L\text{-}H)_2(H_2O)_2]$

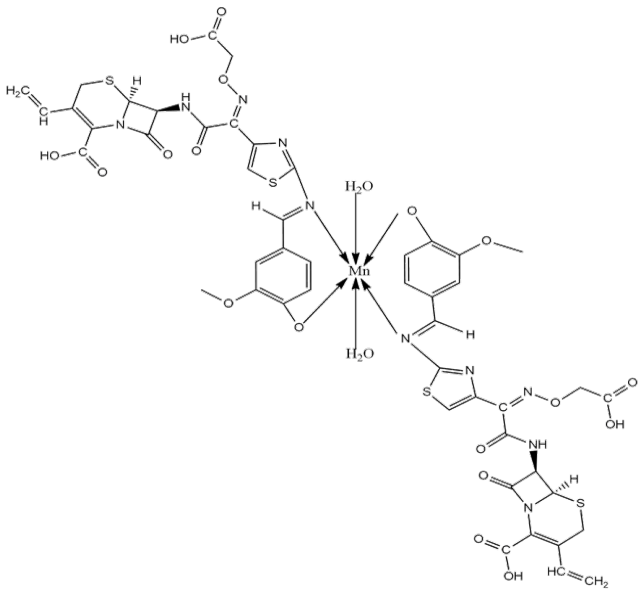

Red solid of $C_{48}H_{58}N_{10}0_{26}S_4Mn$; Yield (76%); M.W (1373.93); UV-Vis (DMSO): 412-465 L-M-OH (π →π*, d→d); FTIR (KBr, cm^{-1}): 1661 (-HC=N), 437 (M-O), 556 (M-N), 3267 (-OH), 1745 (-C=O β-lactam), 1581 (-COO); OCP-OES and Elemental analysis, found (calc.): C 41.99% (41.92%), H 4.29% (4.22%), N 10.24% (10.18%), Mn 4.03% (3.99%)

$[Zn(L\text{-}H)_2(H_2O)_2]$

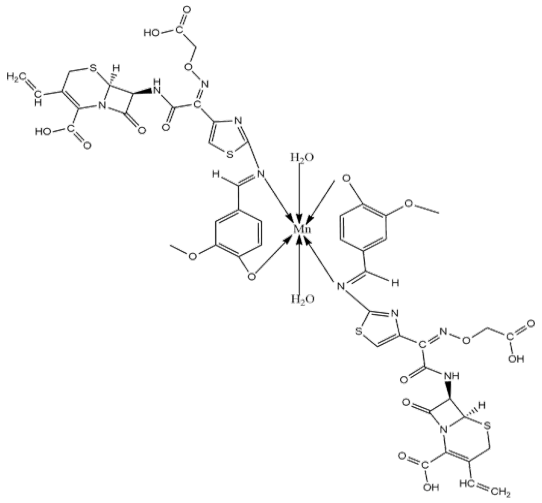

Pinkish solid of $C_{48}H_{58}N_{10}0_{26}S_4Zn$; Yield (72%); M.W (1384.68); UV-Vis (DMSO): 416-472 L-M-OH (π →π*, d→d); FTIR (KBr, cm^{-1}): 1663 (-HC=N), 562 (M-N), 442 (M-O), 3202 (-OH), 1747 (-C=O β-lactam), 1583 (-COO); OCP-OES and Elemental analysis, found (calc.): C 41.64% (41.59%), H 4.26% (4.18%), N 10.21% (10.11%), Mn 4.82% (4.72%)

Biological Studies

Antibacterial Studies

A standard reference approach was adopted to evaluate in-vitro antibacterial activity of the ligand and its metal complexes as well. In-vitro antibacterial investigation was used by employing the disc diffusion technique to examine the biological activity. The ligand and complexes were prepared by dissolving in dimethyl sulfoxide (DMSO) at different concentrations of 100, 50, and 25 mg/mL. Each well on the grass culture plates absorbed around 200 µL of the ligand and its metal complexes at individual doses of 100, 50, and 25 mg/mL, and this indicates that the drug concentration in 10 µL will be 1000, 500, and 250 µg, respectively. The cultural Plates incubation was carried out at 35-37 °C for 17–24 hours after being permitted to stand for one hour to establish appropriate

diffusion. The halo zone of inhibitions surrounding each well was measured in millimeters after incubation. To compute the mean and standard deviation, each sample test was run three times (S.D.).

In-vitro Antioxidant Activity

The Gyamfi *et al.*[13] method, albeit with significant modifications, was employed to examine the complex's ability to scavenge DPPH radicals. To prepare the final solution, 1 mL of the aforementioned solutions was combined with 1mL DPPH solution prepared in DMSO (10 mg in 200 mL). Afterwards, more dimethyl sulfoxide (DMSO) was included to get the solution's volume up to 3 mL. The prepared mixture was mixed vigorously, and later, allowed to rest for approximately 30 minutes at ambient temperature in a lightless environment. At a wavelength of 517 nm, the compounds molar absorbance was measured with Uv-Vis spectrophotometer by using DPPH and DMSO as a reference or blank. To compute the mean and standard deviation, each sample test was run three times (S.D.).[14,15]

The percentage of inhibition was examined by using the below formula.

Inhibition % = (A – B) / A X 100

A= Absorbance of reference, B= Absorbance of sample

The IC50 values calculated by taking three duplicates average.[16-18]

Protease Inhibitory Activities

The peptides or proteins with the ability to block proteolytic enzymes from catalyzing processes are known as protease inhibitors, or PIs. Their extensive dispersion in nature is shown by the fact that they are present in all domains of living life, including viral genomes. The number of genes that encode proteases and protease inhibitors, which make up roughly 2-4% of the genome, indicate the relevance of proteolysis in biological processes. Since the 20th century, these proteases and their inhibitors have been recognized, and protease degradomics has made it simpler to discover them.[19]

Diclofenac sodium was used as a standard for the proteinase inhibition experiment. A 4.55 mL reaction mixture was made by adding 0.120 mg trypsin, 2.0 ml of (40 mM), 0 .55 mL of 50.0 mM Tris-HCl buffer with pH 7.4-7.5 and 2.0 mL of an aqueous solution comprising of test material with a range of concentrations (100-1000 mg/L) that were mixed with the reaction solution. The entire mixture was incubated at 38°C for five minutes. Each sample mixed with 0.5 mL of 1.8% (w/v) casein. The final combination was incubated for an extra 25 minutes. To halt the process, 2.5 mL of perchloric acid with a concentration of 60% was injected to the individual sample. Following the process of centrifugation, the cloudy solution was subjected to measurement of the absorbance of hydrolyzed protein supernatant at a wavelength of 280 nm, with the buffer serving as a reference. The proteinase inhibitory activity was quantified after performing the experiment for three times.[17,20,21] To determine the % inhibition of proteinase inhibitory activity, an additional formula was applied.: proteinase inhibitory (percentage) = (blank absorbance − sample absorbance) ×100/blank absorbance. A linear dosage inhibition curve was obtained by plotting the sample concentration against the corresponding proteinase inhibitory activity, which was utilized to get the IC50 values (concentration giving 50% of proteinase inhibitory effect). In this paper, the inhibition experiment was done by utilizing the trypsin enzyme. To compute the mean and standard deviation, each sample test was run three times (S.D.).[22]

Protein Denaturation

The protein denaturation activity measurement was conducted by following the technique outlined by Gambhir et al., with the incorporation of few modifications proposed by Sakat *et al.*[23]. 4.0mL of saline buffered by phosphates (PBS, pH 6.40) 0.50 mL of products, and 0.050 mL of 0.5% bovine albumin were added to the reaction mixture of volume 5.0 mL and homogenized. After 15-20 minute incubation, the entire mixture was subjected to heating at 75 °C for five minutes in a water bath. After the mixture solutiom had reached a lower temperature, the level of cloudiness was measured at a wavelength of 660.0 nm by using a Shimadzu 2600i spectrophotometer, and the phosphate solution was taken as the reference solution. To determine the level of inhibition of protein denaturation, the following method was utilized where each synthesized Schiff base molecule was assessed at various concentrations between 40 and 250 µg/mL. To compute the mean and standard deviation, each sample test was run three times (S.D.).[24]

To assess the amount of inhibition of protein denaturation, the following formula was employed.

Percent Inhibition of protein denaturation = $(1 - X2/X1) \times 100$

Where X1 = control sample absorbance, and X2 = test sample absorbance.[17]

Results and Discussion

Spectral Data of Ligand and Metal Complexes

Due to the presence of hetro atoms within the ligand structure, we could easily identify the following electronic transitions while examining the UV-Vis spectrum (Figure 4) of the ligand n→π* and π→π*. UV-visible spectra of a ligand containing few bands. One of these bands, at a wavelength of 338nm, is attributed to the emergence of a double bond π →π* transition caused by the -C=N- group. Similarly, at a wavelength of 373 nm, n→π* transitions attributed to second band of lone pair were seen. The confirmation of complex formation was established by the observed shift of metal complex peaks towards higher wavelengths, specifically from 394nm to 430nm. This phenomenon is commonly referred as the charge transfer from the ligand to the metal. The π →π* transition can be attributed to the second visible band in the complex spectra, which appeared in the wavelength range of 440 to 481 nm range. Similarly, the second band appeared in the intricate range of spectra between 410 and 422 nm, resulting from the n →π* transition.

Looking back at the FT-IR spectrum of the freshly synthesized ligand, we can observe clear changes in the absorption bands between the starting materials and the produced molecule. Antibiotic ligands have a variety of donor atoms that can form complexes with transition metal ions. The ligands could have been bound to metal ions via beta-lactam (C=O), thiazine ring (COO), azomethine nitrogen (HC=N), or (C=N-OCH3). An amide is a compound that has a hydroxyl oxygen (-OH) bonded to a carbonyl carbon (C=O). These distinctions include the elimination of the stretching absorption bands of the starting materials' C=O as well as N-H groups due of imine interaction happening through these groups, which results in a unique stretching absorption band at 1600 cm^{-1}, as seen in figures 1-6.

The presence of azomethine nitrogen in the resulting complex with metal ions is confirmed byan absorption band observed at approximately 1620–1665 cm^{-1} in the FTIR-spectra. The azomethine band was observed at 1630 cm^{-1} in the ligand's spectra.[17,18,25,26] The newly found bands at 554-560 cm^{-1} and 430–440 cm^{-1} were attributed to the stretching vibrations of metal–nitrogen (M–N) and metal–oxygen (M–O), respectively. The FT-IR spectra of the related complexes (Figure 2-6) and (Table 1) clearly reveal the existence of coordination through the (C=O) groups of the ligand (carboxylic acid and β-lactam). This is owed to the chemical shifting in the C=O (β-lactam) group's stretching absorption bands compared with the identical band of the ligand by 33 cm^{-1}, 25 cm^{-1}, 34 cm^{-1}, 28 cm^{-1} and 24 cm^{-1} for each of Fe, Cu, Ni, Mn and Zn, respectively, to appear at 1738, 1746, 1737, 1743, 1747 and - cm-1 for each of them. This strong evidence showed that the Schiff base ligands interacted with the metal ions.[27]

Table 1: Spectral Data of the Ligand and its Metal Complexes.

Schiff Base Products	Product Code	UV-Vis (nm) L→M →OH n→π* d→d π →π*		IR (cm^{-1})
Ligand	AL	338	373	1771 (C=O β-lactam), 3376 (OH), 1456 (COO), 1631 (HC=N)
Fe Complex	A1	417	459	1738 (C=O β-lactam), 3214 (OH), 1581 (COO), 1657 (HC=N), 555 (M-N), 436 (M-O)
Cu Complex	A2	422	456	1746 (C=O β-lactam), 3183 (OH), 1590 (COO), 1662 (HC=N), 559 (M-N), 430 (M-O)
Ni Complex	A3	408	452	1737 (C=O β-lactam), 3188 (OH), 1581 (COO), 1657 (HC=N), 436 (M-O), 555 (M-N)
Mn Complex	A4	413	466	1743 (C=O β-lactam), 3265 (OH), 1581 (COO), 1661 (HC=N), 554 (M-N), 435 (M-O)
Zn Complex	A5	415	473	1747 (C=O β-lactam), 3202 (OH), 1582(COO), 1664 (HC=N), 559 (M-N), 4401(M-O)

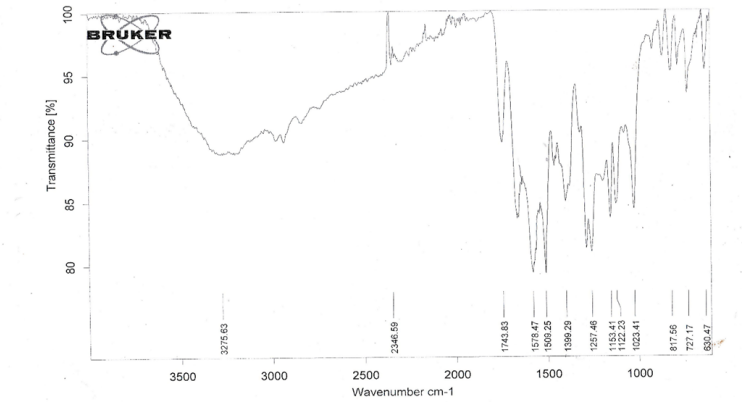

Figure 1: FTIR Spectra of Ligand AL.

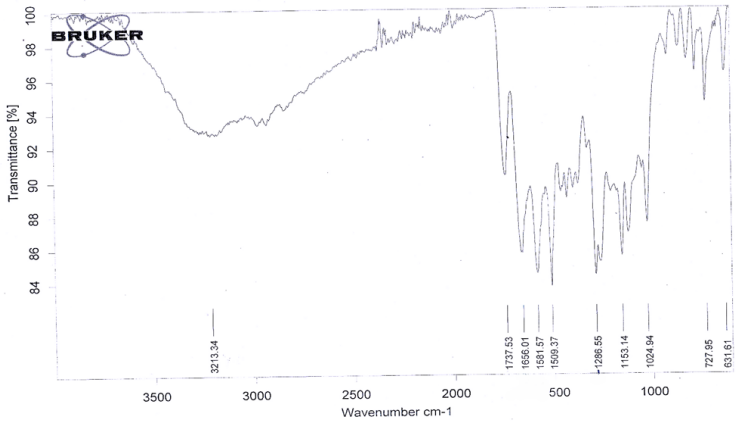

Figure 2: FTIR Spectra of Complex A1.

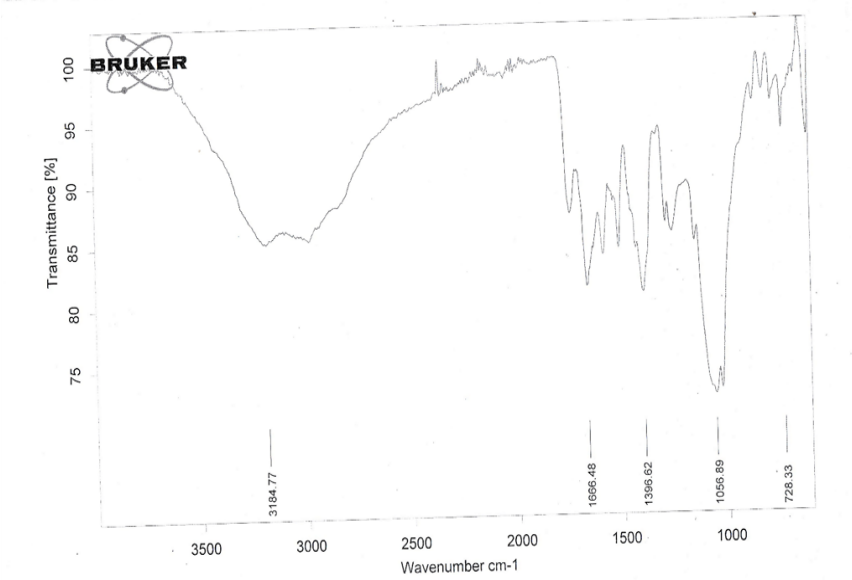

Figure 3: FTIR Spectra of Complex A2.

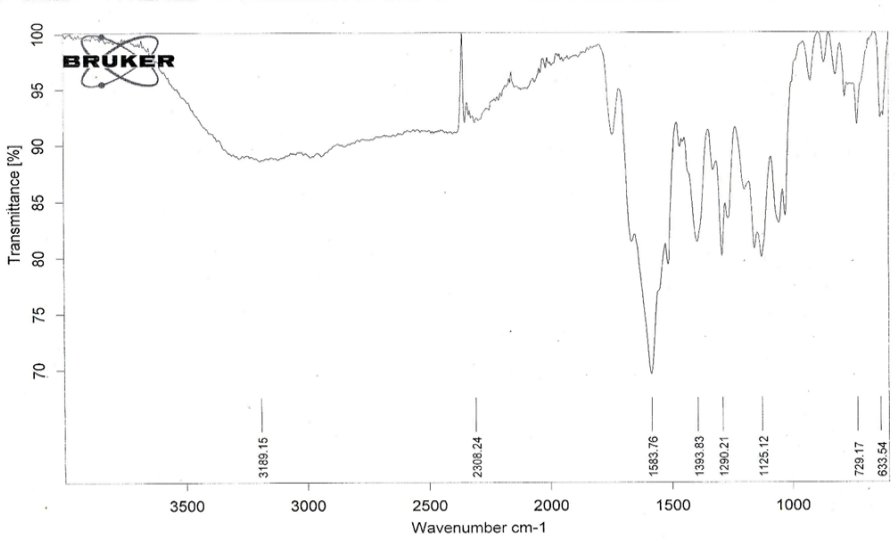

Figure 4: FTIR Spectra of Complex A3.

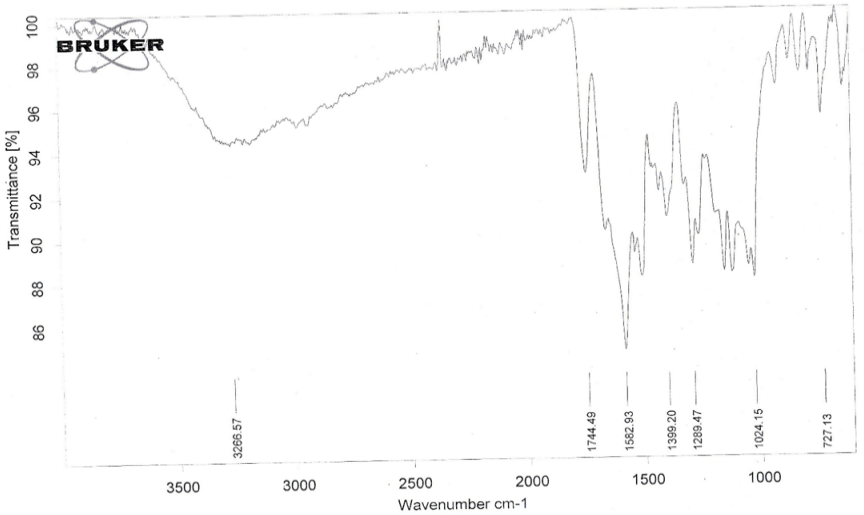

Figure 5: FTIR Spectra of Complex A4.

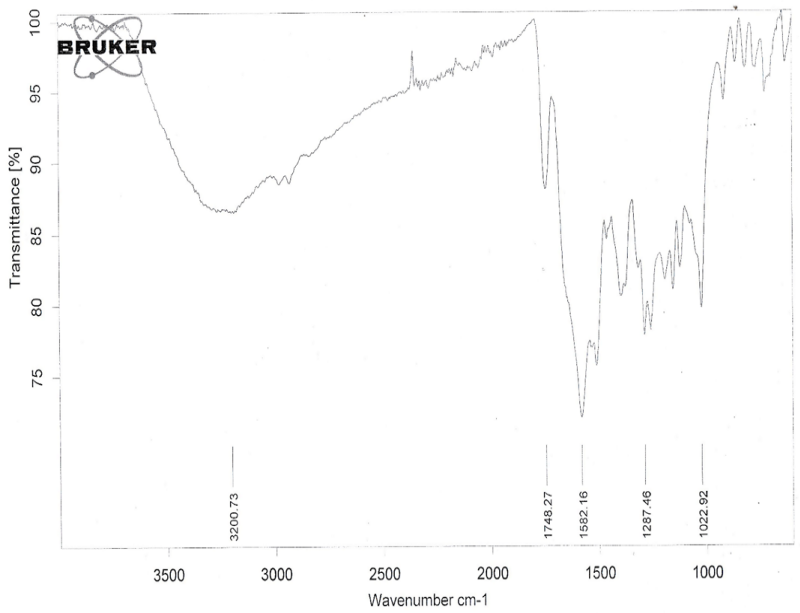

Figure 6: FTIR Spectra of Complex A5.

^{1}H-NMR Spectral Data of Ligand

^{1}H NMR spectrometry was employed to study and confirm the structure of the ligand with DMSO-d6 as the solvent and TMS as the internal standard. The interpreted signals of ^{1}H NMR spectra are of different multiplicity and resonance intensity patterns. In Schiff base ligand spectra, the observed proton signals for the methoxy group are within the range of δ = 3.30-3.91 mg/L.[6]

Since all predicted protons were discovered in their expected zones, the signal appears to verify their hypothesized structure.

The ligand spectra showed a singlet at 8.34 mg/L for the proton of azomethine group (-CH=N) as well as a hydroxy singlet at 9.93 mg/L. A doublet for the methoxy protons was observed at d3 60-3-79 mg/L, whereas the methyl protons were found to be within the range of d 2.45 to 2.48 mg/L. There were multiplets, some overlapping multiplets or doublets present in the aromatic entities range of d6.41 to 8.31 mg/L.[28]

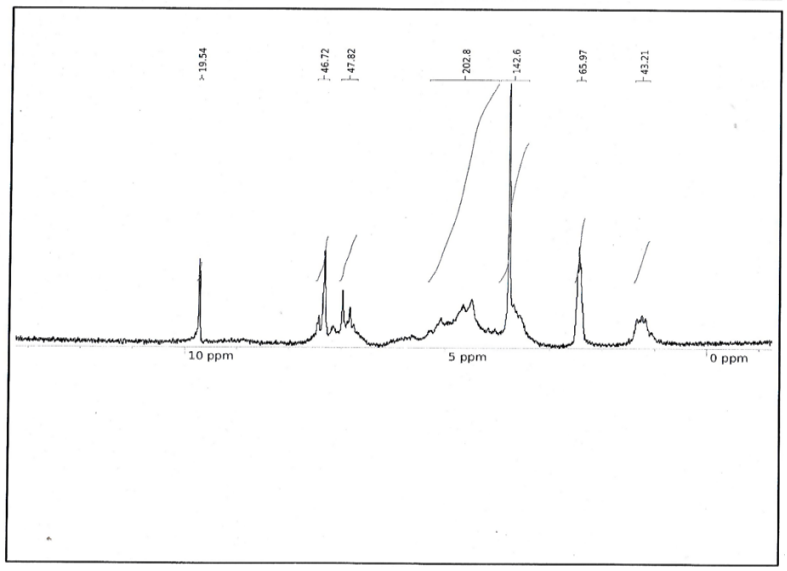

Figure 7: ^{1}H-NMR Spectral Data of Ligand AL.

Studies of X-Ray Diffraction

X-ray diffraction, or XRD for short is a powerful method used to analyze the crystal structure of the materials. The XRD technique was employed to unveil the crystalline properties of the synthesized material. Ultima IV X-Ray Diffractometer (Rigaku CuKα 0.1540562 nm) equipment was employed for the examination of crystalline structures of the compounds

that were synthesized in this work. The selected operating conditions of the instrument were as follows; scanning modes; 2Θ/Θ, continuous scanning, range of scanning: 10°-90°, voltage operating; 40KV, operating current; 30mA. The figure 1-13 are showing the pattern of diffraction for synthesized products. The average particle sizes calculated from graphs were in the range of 33.24 to 64.54 nm, and are reported in the table 2. The maximum grain size obtained was of Zn complex at 64.54 nm and minimum was of Fe complex at 33.24 nm. The particle size and FWHM of Schiff base metal complexes was calculated by applying following Scherrer's equation.

$$P = K\lambda/\beta. \cos\theta$$

Where P represents the crystalline size, K represents the constant having value 0.94, λ represents the X-rays wavelength 0.15, θ represents the diffraction angle, β represents the full width half maximum.[29,30]

Table 2: XRD Particle Size Data of Products.

Products	Size of Particle (nm)	B (FWHM)
A1	33.25	0.28496
A2	50.55	0.27424
A3	48.37	0.25941
A4	39.97	0.28608
A5	61.78	0.13086

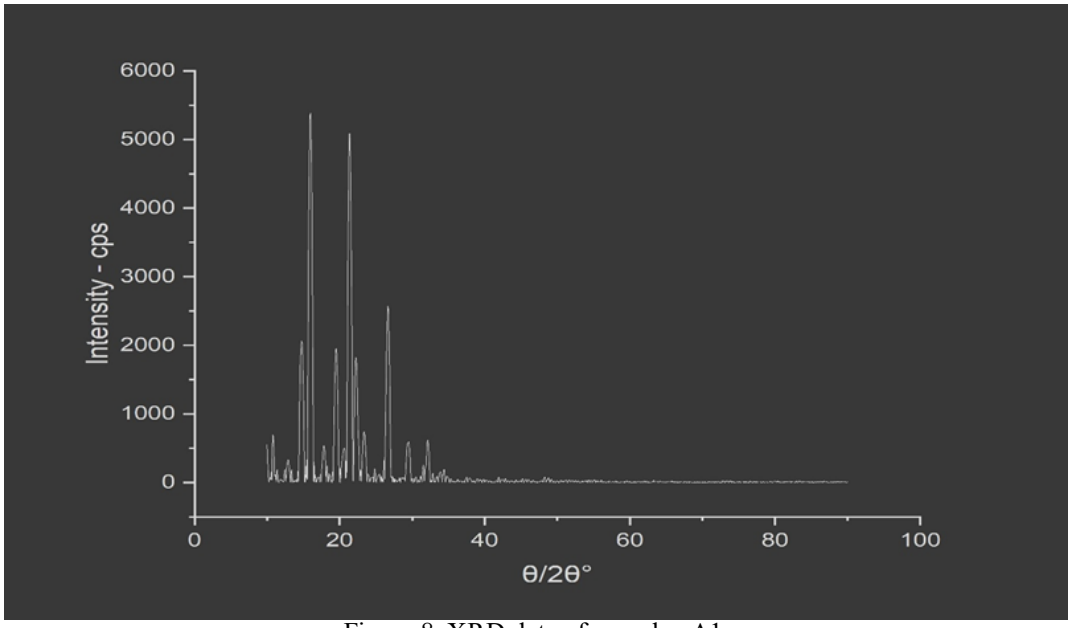

Figure 8: XRD data of complex A1.

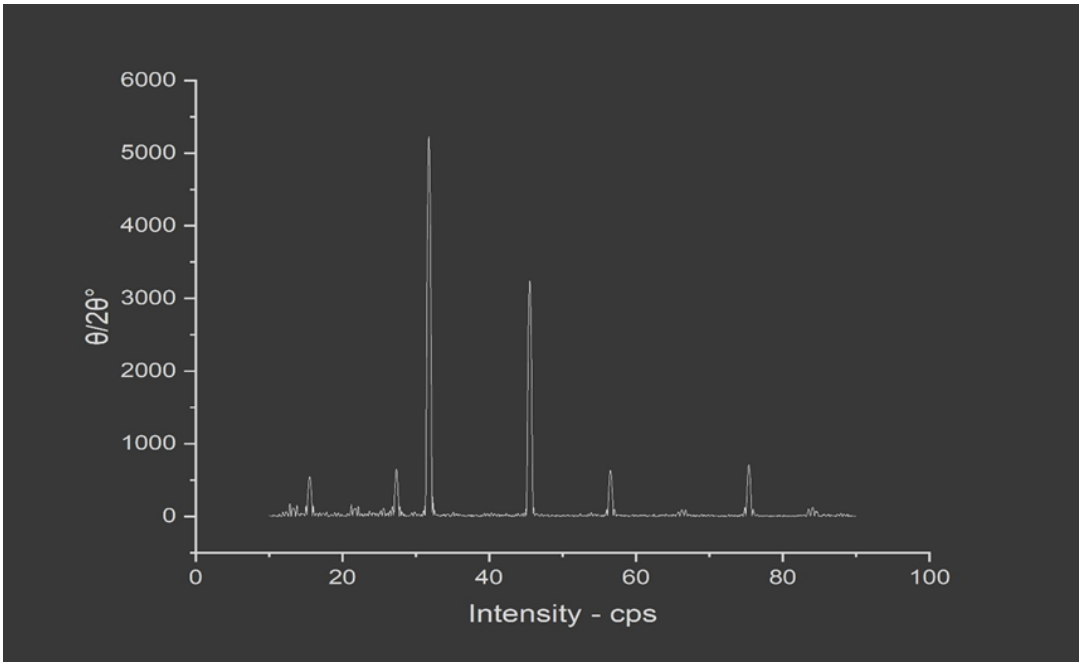

Figure 9: XRD data of complex A2.

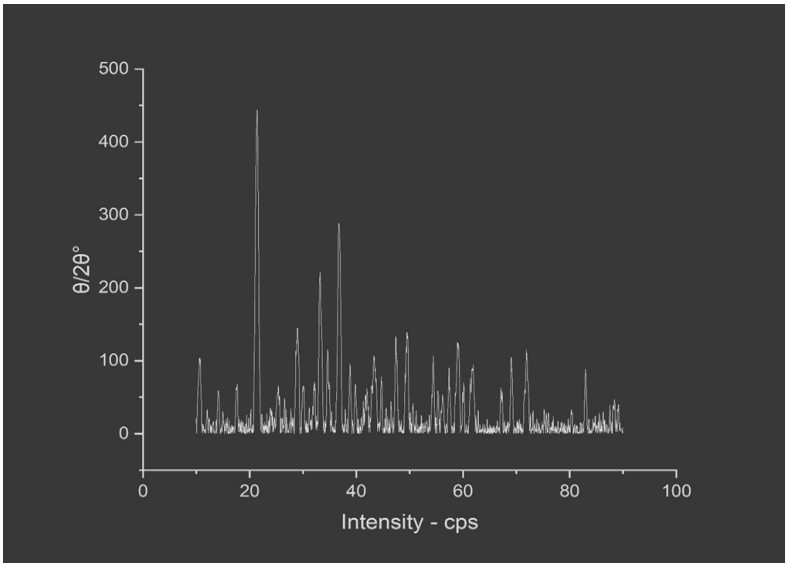

Figure 10: XRD data of complex A3.

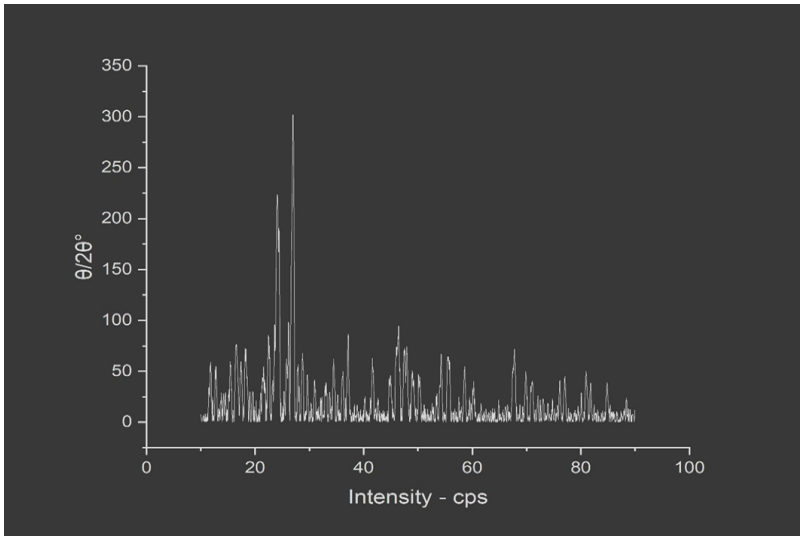

Figure 11: XRD data of complex A4.

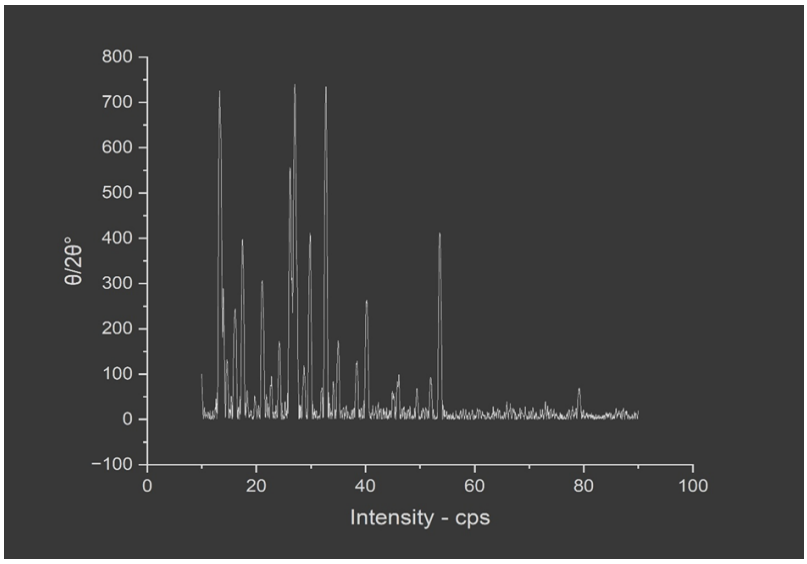

Figure 12: XRD data of complex A5.

Elemental CHN and ICP-OES Metal Analysis of Metal (II) Complexes

For all the complexes of metals (II), the measured percentage data for hydrogen, carbon, nitrogen, and the transition metals (Fe, Mn, Ni, Cu, and Zn) was compared to the values that were calculated from their hypothesized molecular structures. Table 3 presents the computed and obtained values for each complex of metals (II). The metal contents of the complexes were obtained by using an instrument of 7000 Series ICP-OES from Agilent Technologies, USA. All the computational and calculated percentage values were within the allowed range (±0.045-0.38), demonstrating the successful synthesis of the required metal complexes.

Table 3: ICP-OES Metal Content and Elemental Data of Products.

Product		%C	%H	%N	%Fe	%Cu	%Ni	%Mn	%Zn
A1	Found Calc.	45.98 45.87	3.33 3.23	10.21 10.19	4.53 4.41	-	-	-	-
A2	Found Calc.	45.72 45.66	3.24 3.18	11.05 11.01	-	4.88 4.99	-	-	-
A3	Found Calc.	45.91 45.82	3.61 3.50	10.00 11.05	-	-	4.68 4.63	-	-
A4	Found Calc.	45.72 45.61	3.45 3.51	10.25 10.19	-	-	-	4.41 4.35	-
A5	Found Calc.	45.65 45.57	3.27 3.17	10.22 10.12	-	-	-	-	5.22 5.13

Label	Sol'n Conc.	Units	SD	%RSD	Int. (c/s)	Calc Conc.
Fe 238.204	3.13944	ppm	0.078589	2.5	166677	15.13944ppm
Fe 259.940	3.05446	ppm	0.040456	1.3	83219.3	15.05446ppm

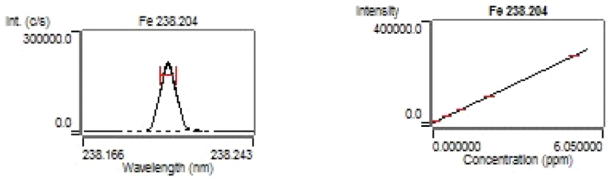

Figure 13: ICP-OES data of Complex A1.

Label	Sol'n Conc.	Units	SD	%RSD	Int. (c/s)	Calc Conc.
Cu 324.754	2.74499	ppm	0.021158	0.8	191017	12.74499ppm
Cu 327.395	2.57863	ppm	0.021812	0.8	104935	12.57863ppm

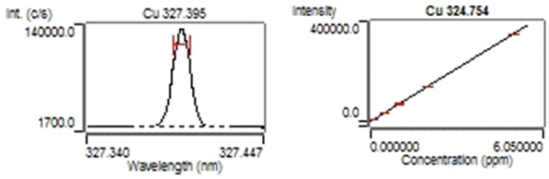

Figure 14: ICP-OES data of Complex A2.

Label	Sol'n Conc.	Units	SD	%RSD	Int. (c/s)	Calc Conc.
Ni 216.555	1.63635	ppm	0.018667	1.1	26242.4	11.63635ppm
Ni 231.604	1.59911	ppm	0.011686	0.7	25510.8	11.59911ppm

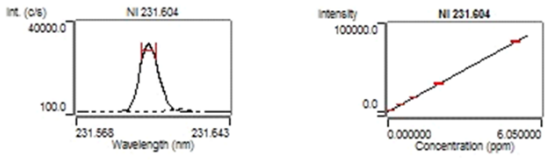

Figure 15: ICP-OES data of Complex A3.

Label	Sol'n Conc.	Units	SD	%RSD	Int. (c/s)	Calc Conc.
Mn 257.610	4.37147	ppm	0.007907	0.2	2309122	14.37147 ppm
Mn 259.372	4.18231	ppm	0.011261	0.3	918632	14.18231ppm

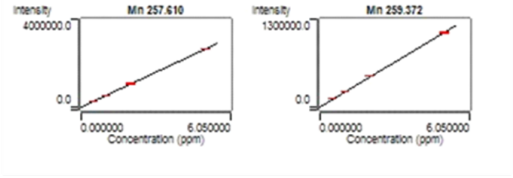

Figure 16: ICP-OES data of Complex A4.

Label	Sol'n Conc.	Units	SD	%RSD	Int. (c/s)	Calc Conc.
Zn 202.548	3.67644	ppm	0.073993	2.0	349993	14.3456 ppm
Zn 213.857	3.66813	ppm	0.029828	0.8	281348	16.5685 ppm

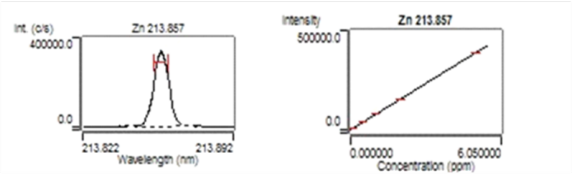

Figure 17: ICP-OES data of Complex A5.

Assessment of in-vitro Antioxidant Activities

The 1,1-diphenyl-2-picryl-hydrazyl (DPPH) analysis was first used as a standard for measuring in vitro radical shielding since it interacts with the chemicals being tested swiftly and consistently. The decline in DPPH values was determined by molar absorbance at the range of 518 nm, and an alteration in the color of the solution reflected the antioxidant's capacity to scavenge radicals by transferring hydrogen radicals or electrons, which produces a stable compound of DPPH-H. For Schiff base ligands and their transition metal (II) complexes, molar absorbance value of DPPH absorbance values at 518 nm were measured in DMSO at varied doses (50, 150, 200, 250, and 300 g/mL) to test the scavenging activity of DPPH radical by using Rutin as a reference drug. This allowed the antioxidant to limit the radical's uptake and alteration in color from purple to yellow. The product inhibition exhibited the dependence on the concentration DPPH radical scavenging activity, with an IC50 value of 302.96±4.18 mg/L and a correlation coefficient (r) of 0.950.[15,18]

Table 4: Ligand and Complexes Antioxidant Activities.

Products	IC50(mg/ml)
AL	0.018
A1	0.28
A2	0.66
A3	0.010
A4	0.093
A5	0.012
Standard	0.016

Standard = Rutin

Proteinase Inhibitory Activity

It has been demonstrated that proteinase inhibitors give substantial resistance. Leukocyte proteinase may have been linked to inflammatory reactions in cases of tissue injury. By using correlation coefficient (r) 0.989 analysis, 435.286 µg/mL was shown to be the IC50 value. The widest inhibition range of Ni complex was observed.[20]

Table 5: Proteinase Inhibitor Activity of Products.

Products	% Inhibition
AL	35%
A1	81%
A2	60%
A3	85%
A4	78%
A5	84%
Standard	61%

Standard= Diclofenac Sodium 52 mg/L

Protein Denaturation

The protein denaturation of the products was suppressed to a percentage range between 19 to 74%. The Mn compound displayed a 78% significant inhibition.

Table 6: Schiff base Compounds Results.

Sample	% Inhibition
AL	28%
A1	71%
A2	24%
A3	62%
A4	35%
A5	78%
Standard	75%

Standard= Diclofenac Sodium 32.5 mg/L

In-Vitro Antibacterial Activity

In-vitro antibacterial investigation was used to examine the biological activity by employing the disc diffusion. Bacterial strains of *Streptococcus pneumonia, Pseudomonas flourescens, Lactobacillus acidophilus, Escherichia coli, Lactococcus cremori, Pseudomonas aeruginosa, Staphylococcus aureus, and Streptococcus pyogenes* were obtained from antibacterial lab of Government College University, Lahore Pakistan. The pure cefixime drug is used as positive standard. The strains were assessed on the nutrient plates against Schiff base and the derivatives.

Table 7: Antibacterial Activity Data of Products.

Sample	S.pneumoniae	S.Aureus	P.aeruginosa	E.Coli	L.acidophilus	S.Fluorescens	L.Cremoris	S.Pyogenes	Standard Deviation
AL	12	13	15	12	18	15	18	13	2.45
A1	24	23	21	22	25	21	18	20	2.25
A2	21	-	23	20	20	13	-	22	3.55
A3	-	21	22	-	18	22	28	25	3.45
A4	18	17	19	25	19	17	23	19	2.87
A5	-	19	21	26	21	18	24	-	3.02

Molecular Docking Studies

Molecular Docking studies were performed with the complexes A1, A2, A3, A4, A5, ligand AL and the standard drug (Cefixime) by using PyRx-Virtual Screening Tool on the protein with the crystal structure of GlcN-6-P synthase (PDB ID-1MOQ) for antibacterial activity. The structure of protein was retrieved from https://www.rcsb.org/structure/1MOQ for antibacterial study, and the protein purification was carried out by using *Discovery Studio Visualizer 4.5* software. All the co-crystallized ligands, water molecules, and other complexes were abstracted from the protein structure. The preparation of ligands was carried out by using ChemDraw Professionals 15.0 and MarvinSketch 5.11.0. In the present study, the ligand and the complexes were converted into two-dimensional (2D) and three-dimensional (3D) structures by using the build and optimize procedure, and the resulting 3D structures were saved in PDB format. This initial step involved the preparation of the ligand molecules, where parameters such as bond orders, hybridization charges, free hydrogens, and flexible torsions were assigned. The generated 3D structures were later imported into the PyRx-Virtual Screening Tool for docking analysis. The docking was carried out by using the Vina Wizard, and the binding affinity scores were determined in kcal/mol. The accuracy of these predictions normally depends on the scoring functions used to evaluate the complementarity between the ligand and the receptor.

On the basis of experimental data, complexes A1, A2, A3, A4, A5, ligand AL and Cefixime (standard drug) were docked in PyRx-Virtual Screening Tool by using protein with PDB ID-1MOQ (Figure 19-21). The structures of all the complexes A1, A2, A3, A4, A5, ligand AL and standard drug (Cefixime) with binding affinity scores are shown in the Table 8. Although, all the ligands were found to have excellent outcomes; however, out of complexes A1, A2, A3, A4, A5, ligand AL and Cefixime (standard drug), complex A5 for antibacterial was found to have very potent activity. The docking output of complexes A1, A2, A3, A4, A5, ligand AL and Cefixime as standard drug is mentioned in Table 8.

All of the complexes A1, A2, A3, A4, A5, ligand AL, and Cefixime (the standard drug) were allocated inside Vina Wizard. The relevant software was then used to assign the important bonds, bond order, hybridization, polar charges, etc. within Autodock wizard. The process of ligand docking involved the formation of many conformations of the ligand within the hotspot. It is important to record the scores of these diverse conformations within the binding pocket since they support distinct interactions between the ligand and the receptor. Non-covalent intermolecular interactions, such as hydrogen bonds between molecules, hydrophobic contacts, Vander Waal contacts, and electrostatic contacts, primarily affect binding affinity. Similarly, the presence of several chemical molecules may also affect the binding affinity between a ligand and the hotspot of the receptor.

The protein-ligand interaction studies are accompanied by the results of molecular docking. The results of protein-ligand interaction with the reference medication, cefixime, have been tabulated to demonstrate the number of hydrogen bonding, amino acid interactions, and binding affinity score (Figure 19). Stable binding contact between ligands and receptors is demonstrated by the ligand's negative binding energies. The complexes A1, A2, A3, A4, A5, and ligand AL are docked in this work by using PDB (1MOQ) and cefixime as the reference medication. With the exception of A3, all the tested complexes for anti-bacterial activity demonstrated higher binding affinity scores than the reference medication, cefixime. Complex A5, which has a binding energy of -8.9 kcal/mol, was shown to have the most powerful antibacterial activity among the complexes A1, A2, A3, A4, A5 and ligand AL based on hydrogen bond interactions. In addition to some intramolecular hydrogen bonding between complex A5 and binding site (1MOQ) with bond lengths of 2.12, 2.27, and 2.40 Å, four hydrogen bonding contacts were identified as His493, Val399, Thr352, Thr302, and Thr353 with bond lengths of 2.80, 2.67, 3.03, and 2.44 Å, respectively. The hydrophobic interactions between the amino acid residues Tyr304, Lys487, and Lys487 were also observed between complex A5 and hotspot (1MOQ).

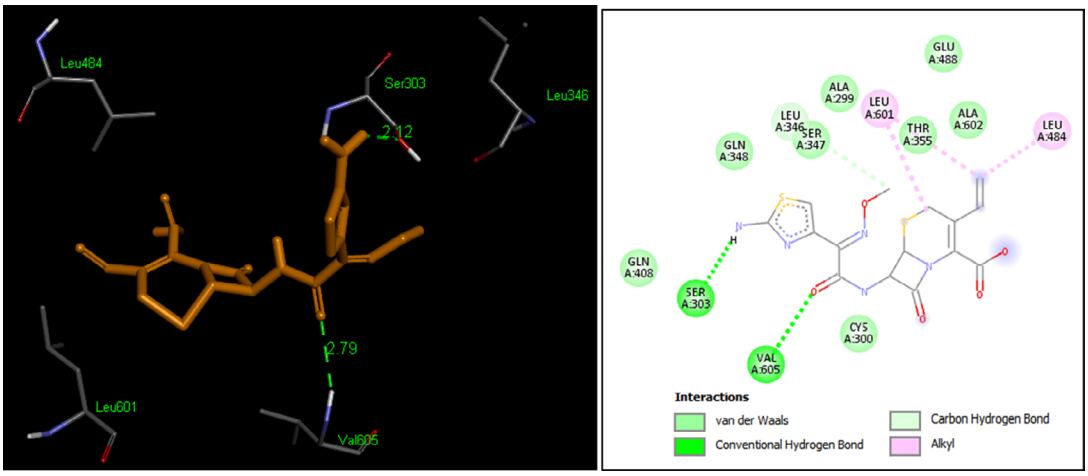

Figure 18: 3D (Left) and 2D (Right) Binding Contacts of Standard Drug (Cefixime).

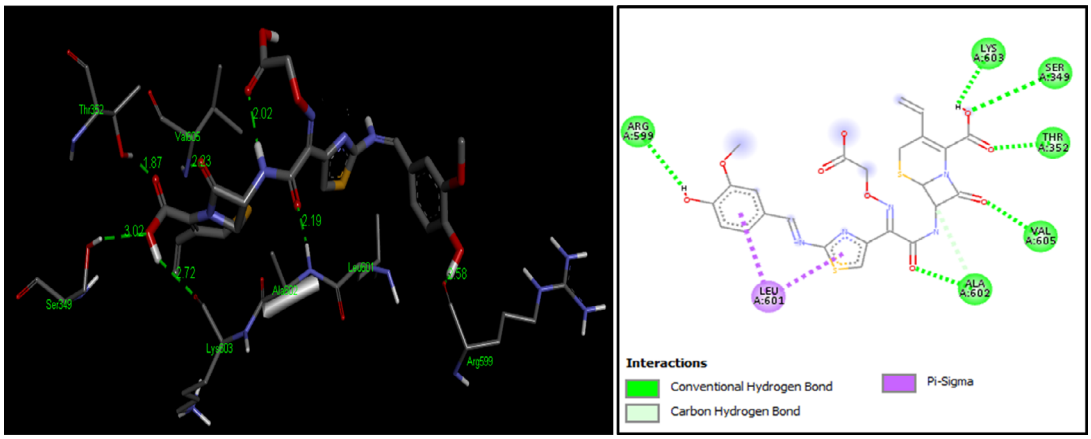

Figure 19: 3D (Left) and 2D (Right) Binding Interactions of Ligand AL.

The obtained data demonstrated that every ligand under investigation had a similar orientation and location within the protein's putative hotspot, which serves as a route for the substrate to transfer from the hotspot to the hotspot. Strong evidence links the ligand's affinity for protein to the binding of free energy, which may help to understand and provide an explanation for the ligand's action through a variety of potential pathways. Similarly, ligand-receptor complex shape plays a crucial role in determining the therapeutic action. This *in silico* work also provides a valuable perspective for researchers looking for new drugs with effective antibacterial activity. The thiazole ring, (S)-5-thia-1-azabicyclo [4.2.0] oct-2-ene ring, and aromatic ring might be closely associated with the protein mentioned above, and the data suggests that the proximate compounds should be synthesized for further investigation.

Table 8: Docking of Ligands A1–A5, AL and Standard Drug (Cefixime) to GlcN-6-P Synthase (PDB ID: 1MOQ) using *PyRx*.

Compd. No.	[a]Binding Affinity (Kcal/mol)	[b]Hydrogen Bonding	Distances (Å)	Hydrophobic Interactions
A1	-7.3	Asn^{305}, Lys^{487}, Tyr^{312}	2.05, 2.80, 2.42, 2.75[c], 2.54[c], 2.94[c], 2.50[c], 2.08[c], 1.88[c], 1.84[c], 1.75[c]	Leu^{484}, Tyr^{437}, Ala^{498}, Ala^{498}, Tyr^{497}, Arg^{472}
A2	-7.6	His^{493}, Lys^{487}, Gly^{301}, Tyr^{304}, Tyr^{304}, Val^{324}, Val^{324}, Cys^{322}	2.30, 2.85, 2.32, 2.94, 2.62, 2.64, 2.43, 2.88, 2.62[c], 2.94[c], 2.23[c], 2.22[c], 1.89[c], 1.99[c], 1.88[c], 3.24[c], 3.23[c]	Tyr^{304}, Ile^{326}, Leu^{484}
A3	-5.9	Arg^{270}, Thr^{268}, Asn^{392}, Asn^{392}, Asn^{375}	2.57, 2.37, 3.06, 2.91, 2.33, 2.38[c], 2.38[c], 2.14[c], 2.91[c], 1.89[c], 1.86[c], 3.39[c], 2.93[c], 2.73[c]	Pro^{377}, Met^{390}
A4	-7.5	-	3.06[c], 2.08[c], 2.05[c], 1.72[c], 1.67[c], 1.43[c]	-
A5	-8.9	His^{493}, Val^{399}, Thr^{352}, Thr^{302}	2.80, 2.67, 3.03, 2.44, 2.12[c], 2.27[c], 2.40[c]	Tyr^{304}, Lys^{487}, Lys^{487}
AL	-7.8	Arg^{599}, Leu^{601}, Lys^{603}, Ser^{349}, Thr^{352}, Val^{605}	2.58, 2.19, 2.72, 3.02, 1.87, 2.23, 2.02[c]	Leu^{601}, Leu^{601}
Cefixime (Std.)	-7.3	Ser^{303}, Val^{605}	2.12, 2.79	Gln^{408}, Ser^{347}, Ala^{299}, Glu^{488}, Ala^{602}, Thr^{355}, Cys^{300}

[a]Computed from the docked position using PyRx's ligand contact tool. [b]Hydrogen bond length determined using PyRx's Ligand contact tool from docked position. [c]Hydrogen bonding within molecules.

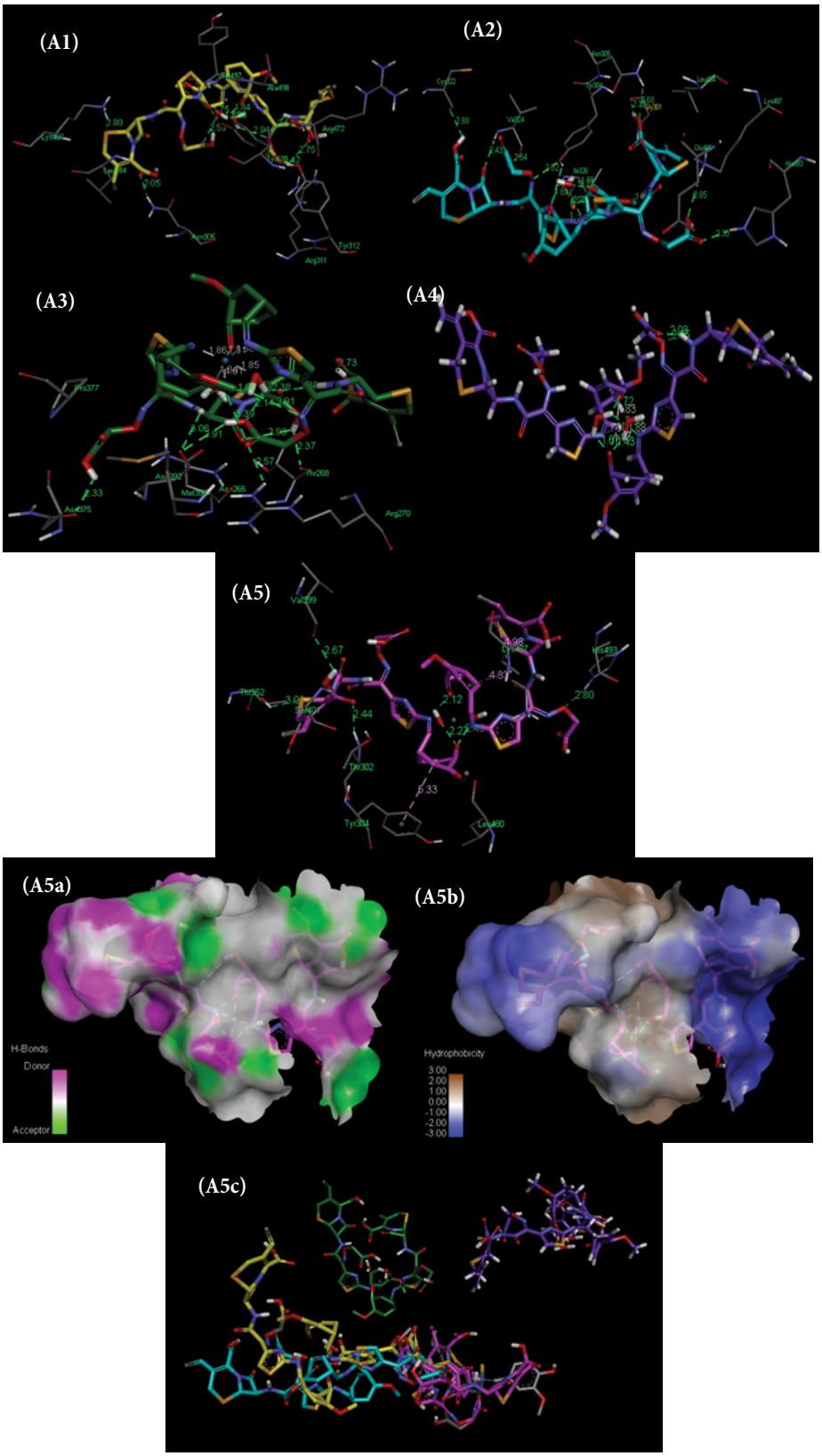

Figure 20: 3D Conformations of the Docked Ligands A1, A2, A3, A4, and A5, Displaying Interactions Inside the GlcN-6-P synthase's Binding Pocket (PDB ID: 1MOQ). A5a) Representing Hydrogen Bond Analysis (left) and, A5b) Showing Hydrophobic Interaction Analysis (right) of Ligand A5. The hydrophobic Contacts' Blue Colour Denotes Favourable Structural Features (atoms and torsions) that Contribute to the GlcN-6-P Synthase's (PDB ID: 1MOQ) Overall Binding Energy; the Pink and White Colors are Unfavorable and Neutral, respectively. A5c) Describes the Overlap Diagram for the Ligand AL and the Five Complexes A1, A2, A3, A4, and A5.

The cefixime–vanillin–Zn Schiff base metal complex A5 shows the strongest activity because vanillin's aromatic, hydroxyl, and methoxy groups provide extended conjugation, hydrogen-bonding ability, and π–electron interactions. These features, combined with Schiff base formation and Zn^{2+} chelation, greatly enhance lipophilicity, membrane permeability, binding affinity, and biological stability — amplifying cefixime's inherent antimicrobial power. The imine group can improve interaction with biological receptors and facilitate coordination with metal ions. This modification often enhances penetration across microbial cell membranes, leading to stronger antimicrobial activity.

Conclusion

In this study, Schiff base ligand was synthesized by treating cefixime with an aromatic aldehyde, vanillin. A range of analysis approaches, such as spectroscopic, elemental and structural were applied to characterize all the products. The biological activities were evaluated and according to the findings, metal complexes are biologically more effective than both their free ligands and equivalent parent medicines. *In silico* experiments were also conducted, and based on hydrogen bond interactions, complex A5, having a binding energy of -8.9 kcal/mol, was observed to have the strongest antibacterial activity among complexes A1, A2, A3, A4, A5, and ligand AL. The above-described protein GlcN-6-P synthase (PDB ID-1MOQ) may be closely related to the thiazole ring, (S)-5-thia-1-azabicyclo [4.2.0] oct-2-ene ring, and aromatic ring; the data suggests that the more derivative complexes should be synthesized and studied for additional research.

Acknowledgements

Researchers would like to thank Deanship of scientific research, Qassim University, Saudi Arabia, for funding the publication of this project.

References

1. Refat MS, Altalhi T, Fetooh H, Alsuhaibani AM, Hassan RF. In neutralized medium five new Ca(II), Zn(II), Fe(III), Au(III) and Pd(II) complexity of ceftriaxone antibiotic drug: Synthesis, spectroscopic, morphological and anticancer studies. J Mol Liq. 2021; 322: 114816. doi: https://doi.org/10.1016/j.molliq.2020.114816.
2. Zabiszak M, Frymark J, Ogawa K, et al. Complexes of β-lactam antibiotics and their Schiff-base derivatives as a weapon in the fight against bacterial resistance. Coord Chem Rev. 2023; 493: 215326. doi: https://doi.org/10.1016/j.ccr.2023.215326.
3. Boulechfar C, Ferkous H, Delimi A, et al. Schiff bases and their metal Complexes: A review on the history, synthesis, and applications. Inorg Chem Commun. 2023; 150: 110451. doi: https://doi.org/10.1016/j.inoche.2023.110451.
4. Uddin MN, Ahmed SS, Alam SMR. REVIEW: Biomedical applications of Schiff base metal complexes. J Coord Chem. 2020; 73(23): 3109-49. doi: https://doi.org/10.1080/00958972.2020.1854745.
5. Ashraf T, Ali B, Qayyum H, Haroone MS, Shabbir G. Pharmacological aspects of schiff base metal complexes: A critical review. Inorg Chem Commun. 2023; 150: 110449. doi: https://doi.org/10.1016/j.inoche.2023.110449.
6. Naureen B, Miana GA, Shahid K, Asghar M, Tanveer S, Sarwar A. Iron (III) and zinc (II) monodentate Schiff base metal complexes: Synthesis, characterisation and biological activities. J Mol Struct. 2021; 1231: 129946. doi: https://doi.org/10.1016/j.molstruc.2021.129946.
7. Chaudhary NK, Guragain B, Chaudhary SK, Mishra P. Schiff base metal complex as a potential therapeutic drug in medical science: A critical review. Bibechana. 2021; 18(1): 214-30. doi: https://doi.org/10.3126/bibechana.v18i1.29841.
8. Makinta AS, Fugu MB, Naomi NP, Mahmud MM, Ahmed AA. Physicochemical Characterization and Antimicrobial Activity of Mechanochemically and Solvent-Based Synthesized Mn(II) Complexes of Cefixime and Cefuroxime. Chem Rev Lett. 2022; 5(4): 261-67. doi: https://doi.org/10.22034/crl.2022.330636.1157.
9. Umekar MJ, Lohiya RT, Gupta KR, Kotagale NR, Raut NS. Studies on meropenem and cefixime metal ion complexes for antibacterial activity. Futur J Pharm Sci. 2021; 7(1): 233. doi: https://doi.org/10.1186/s43094-021-00379-0.
10. Ceramella J, Iacopetta D, Catalano A, Cirillo F, Lappano R, Sinicropi MS. A Review on the Antimicrobial Activity of Schiff Bases: Data Collection and Recent Studies. Antibiotics (Basel). 2022; 11(2): 191. doi: https://doi.org/10.3390/antibiotics11020191.
11. Venkatesh G, Vennila P, Kaya S, et al. Synthesis and Spectroscopic Characterization of Schiff Base Metal Complexes, Biological Activity, and Molecular Docking Studies. ACS Omega. 2024; 9(7): 8123-38. doi: https://doi.org/10.1021/acsomega.3c08526.
12. Sathyanarayana et al. vanillin Schiff base Cu(II)/Zn(II) complexes showed significant activity against S. aureus and E. coli. 2019.
13. Gyamfi MA, Yonamine M, Aniya Y. Free-radical scavenging action of medicinal herbs from Ghana: Thonningia sanguinea on experimentally-induced liver injuries. Gen Pharmacol. 1999; 32(6): 661-7. doi: https://doi.org/10.1016/s0306-3623(98)00238-9.
14. Yadav M, Sharma S, Devi J. Designing, spectroscopic characterization, biological screening and antioxidant activity of mononuclear transition metal complexes of bidentate Schiff base hydrazones. J Chem Sci. 2021; 133(1): 21. doi: https://doi.org/10.1007/s12039-020-01854-6.
15. Al-Amiery AA, Kadhum AA, Mohamad AB. Antifungal and antioxidant activities of pyrrolidone thiosemicarbazone complexes. Bioinorg Chem Appl. 2012; 2012: 795812. doi: https://doi.org/10.1155/2012/795812.
16. Sekhar EV, Karki SS, Rangaswamy J, Bhat M, Kumar S. Synthesis, characterization, and biological evaluation of some 4-((thiophen-2-yl-methylene)amino) benzenesulfonamide metal complexes. Beni-Suef Univ J Basic Appl Sci. 2021; 10(1): 28. doi: https://doi.org/10.1186/s43088-021-00113-y.

17. Gulalkari RA. Preparation, Characterization and Pharmacological evaluation of Bauhinia variegata Lauha Bhasma. Research Journal of Pharmacy and Technology. 2022; 15(11): 5295-301. doi: https://doi.org/10.52711/0974-360X.2022.00892.
18. Turan N, Buldurun K, Türkan F, et al. Some metal chelates with Schiff base ligand: synthesis, structure elucidation, thermal behavior, XRD evaluation, antioxidant activity, enzyme inhibition, and molecular docking studies. Mol Divers. 2022; 26(5): 2459-72. doi: https://doi.org/10.1007/s11030-021-10344-x.
19. Mohan M, Kozhithodi S, Nayarisseri A, Elyas KK. Screening, Purification and Characterization of Protease Inhibitor from Capsicum frutescens. Bioinformation. 2018; 14(6): 285-93. doi: https://doi.org/10.6026/97320630014285.
20. Singh A, Malhotra D, Singh K, Chadha R, Bedi PMS. Thiazole derivatives in medicinal chemistry: Recent advancements in synthetic strategies, structure activity relationship and pharmacological outcomes. J Mol Struct. 2022; 1266: 133479. doi: https://doi.org/10.1016/j.molstruc.2022.133479.
21. Głowacka IE, Grabkowska-Drużyc M, Andrei G, et al. Novel N-Substituted 3-Aryl-4-(diethoxyphosphoryl) azetidin-2-ones as Antibiotic Enhancers and Antiviral Agents in Search for a Successful Treatment of Complex Infections. Int J Mol Sci. 2021; 22(15): 8032. doi: https://doi.org/10.3390/ijms22158032.
22. Assiry AA, Bhavikatti SK, Althobaiti FA, Mohamed RN, Karobari MI. Evaluation of In Vitro Antiprotease Activity of Selected Traditional Medicinal Herbs in Dentistry and Its In Silico PASS Prediction. Biomed Res Int. 2022; 2022: 5870443. doi: https://doi.org/10.1155/2022/5870443.
23. Sakat S, Juvekar AR, Gambhire MN. In vitro Antioxidant and Anti-Inflammatory Activity of Methanol Extract of Oxalis corniculata Linn. Int J Pharm Pharm Sci. 2010; 2(1): 146-55. Available from: https://innovareacademics.in/journal/ijpps/Vol2Issue1/322.pdf.
24. Hamid SJ, Salih T. Design, Synthesis, and Anti-Inflammatory Activity of Some Coumarin Schiff Base Derivatives: In silico and in vitro Study. Drug Des Devel Ther. 2022; 16: 2275-88. doi: https://doi.org/10.2147/dddt.s364746.
25. Raman N, Thangaraja C, Johnsonraja S. Synthesis, spectral characterization, redox and antimicrobial activity of Schiff base transition metal(II) complexes derived from 4-aminoantipyrine and 3-salicylideneacetylacetone. Central European Journal of Chemistry. 2005; 3(3): 537-55. doi: https://doi.org/10.2478/BF02479281.
26. Abd-Elzaher MM. Spectroscopic Characterization of Some Tetradentate Schiff Bases and Their Complexes with Nickel, Copper and Zinc. J Chin Chem Soc. 2001; 48(2): 153-58. doi: https://doi.org/10.1002/jccs.200100027.
27. Golcu A, Tumer M, Demirelli H, Wheatley RA. Cd(II) and Cu(II) complexes of polydentate Schiff base ligands: synthesis, characterization, properties and biological activity. Inorganica Chim Acta. 2005; 358(6): 1785-97. doi: https://doi.org/10.1016/j.ica.2004.11.026.
28. Breitmaier E. Structure Elucidation by NMR in Organic Chemistry: A Practical Guide. John Wiley & Sons; 2002. doi: https://doi.org/10.1002/0470853069.
29. Chellaian JD, Salin Raj SS. Co(II), Ni(II), Cu(II), and Zn(II) complexes of 4-aminoantipyrine-derived Schiff base. Synthesis, structural elucidation, thermal, biological studies, and photocatalytic activity. J Heterocycl Chem. 2021; 58(4): 928-41. doi: https://doi.org/10.1002/jhet.4209.
30. Kazar AR. Synthesis, characterization of Co3O4 and NiO metal oxide nanoparticles using metal Schiff base complexes as precursor A project. Council of the College of Science for Women, University of Babylon; 2023. Available from: https://cdnx.uobabylon.edu.iq/undergrad_projs/QA0FmQujkC00mxYSH7ww.pdf.